Application of Image Texture Analysis for Online Determination of Curd Moisture and Whey Solids in a Laboratory-Scale Stirred Cheese Vat

C.C. Fagan, C.-J. Du, C.P. O'Donnell, M. Castillo, C.D. Everard, D.J. O'Callaghan, and F.A. Payne

ABSTRACT: A noninvasive technology, which could be employed online to monitor syneresis, would facilitate the production of higher quality and more consistent cheese products. Computer vision techniques such as image texture analysis have been successfully established as rapid, consistent, and nondestructive tools for determining the quality of food products. In this study, the potential of image texture analysis to monitor syneresis of cheese curd in a stirred vat was studied. A fully randomized 2-factor (milk pH and stirring speed), 2-level factorial design was carried out in triplicate. During syneresis, images of the surface of the stirred curd–whey mixture were captured using a computer vision system. The images were subjected to 5 image texture analysis methods by which 109 image texture features were extracted. Significant correlations were observed between a number of image texture features and curd moisture and whey solids. Multiscale analysis techniques of fractal dimension and wavelet transform were demonstrated to be the most useful for predicting syneresis indices. Fractal dimension features predicted curd moisture and whey solids during syneresis with standard errors of prediction of 1.03% (w/w) and 0.58 g/kg, respectively. It was concluded that syneresis indices were most closely related to the image texture features of multiscale representation. The results of this study indicate that image texture analysis has potential for monitoring syneresis.

Keywords: computer vision, curd moisture, image processing, image texture, syneresis, whey solids

Introduction

Syneresis is the process in cheese making whereby whey is expelled from curd particles, which are then separated from the whey by drainage and undergo further processing steps before producing a cheese product. Control of the rate and extent of syneresis is vital because deviations from optimum moisture content by as little as 1% can detrimentally affect cheese ripening, yield, and therefore quality and profits (Emmons 1993; Fagan and others 2007a). In general, syneresis is empirically controlled by the processor by varying process conditions such temperature or coagulum cutting time. However, with the current trend toward upscaling and increased automation of the cheese-making process, a rapid, online, and nondestructive method of monitoring syneresis is seen as highly desirable. Indeed, Woodcock and others (2008) stated that the implementation of a process analytical technology (PAT) system, which is a system for designing, analyzing, and controlling manufacturing through timely measurements of critical quality and performance attributes of raw and inprocess materials, in cheese manufacture would assist in achieving a consistently high-quality product. Several technologies have been investigated as PAT tools in cheese manufacture, including infrared spectroscopy (Blazquez and others 2004; Fagan and others 2007b).

MS 20070823 Submitted 11/6/2007, Accepted 2/25/2008. *Authors Fagan and O'Donnell are with Biosystems Engineering, UCD School of Agriculture, Food Science and Veterinary Medicine, Univ. College Dublin, Earlsfort Terrace, Dublin 2, Ireland. Author Du is with Computer Vision and Imaging Research Group, School of Computing, Univ. of Dundee, Dundee DD1 4HN, Scotland. Authors Castillo and Payne are with Dept. of Biosystems and Agricultural Engineering, 128 C. E. Barnhart Building, Lexington, KY 40546-0276, U.S.A. Authors Everard and O'Callaghan are with Moorepark Food Research Centre, Teagasc, Fermoy, Co. Cork, Ireland. Direct inquiries to author Fagan (E-mail: colette.fagan@ucd.ie).*

As a rapid, consistent, nondestructive, and objective tool, computer vision has been successfully established as a technique for quality inspection of food products (Mendoza and Aguilera 2004; Misimi and others 2007), including cheese. Apostolopoulos and Marshall (1994) developed a computer vision method to determine the shreddability of cheese and found good correlation between shreddability as measured by image analysis and by sensory evaluation. In the study of Ni and Gunasekaran (1995), cheese shred dimensions were determined from skeletonized images using syntactic networks, which successfully recognized individual shreds when two were in contact or overlapping, and results compared well with manual measurements. The meltability, browning, and oiling off properties of Cheddar and Mozzarella cheeses were investigated under different cooking conditions and sizes of sample using computer vision (Wang and Sun 2002). Recently, computer vision techniques have been extended to the inspection of the distribution and amount of ingredients in pasteurized cheese (Jeliński and others 2007).

Image texture is an important feature extracted from food images for characterizing properties such as smoothness, coarseness, and graininess. Recently, a variety of image texture analysis methods have been applied to food quality inspection. The most popular approaches are the gray level co-occurrence matrix (GLCM), the run-length matrix (RLM), the 1st-order gray level statistics (FGLS), the fractal dimension (FD), Fourier transform (FT), and wavelet transform (WT) based methods (Du and Sun 2004). Transform-based texture analysis techniques (FT and WT) determine the texture of an object by converting the image into a new form using the spatial frequency properties of the pixel intensity variations. The WT performs a space-frequency decomposition of an image and is more suitable for texture analysis than FT, which only performs frequency decomposition.

doi: 10.1111/j.1750-3841.2008.00814.x

The majority of applications of image texture analysis in food are for beef quality evaluation (Whittaker and others 1992; McCauley and others 1994; Shiranita and others 1998; Li and others 1999, 2001). Image texture features are also feasible for discriminating between abnormal and normal poultry carcasses (Park and Chen 1996), describing the microstructure of potato cells (Quevedo and others 2002), and classifying cereal grains (Majumdar and Jayas 2000). However, image texture analysis has not been applied to cheese quality control during manufacture.

Everard and others (2007) have applied computer vision to monitor curd syneresis in a cheese vat. They extracted the average RGB (red, green, and blue) values from images and obtained the areas of curd and whey using a thresholding-image segmentation technique. Although the technique was found to distinguish between the effect of pH and stirring speed, they stated that the low stirring speed in their study confounded the prediction of curd moisture. Fagan and others (2007c, 2007d, 2008) investigated the potential of a submerged near-infrared sensor installed on the wall of a cheese vat for monitoring syneresis and predicting indices such as curd moisture content during syneresis. They found that the sensor response was sensitive to changes in curd moisture and whey fat content during syneresis (Fagan and others 2007c) and that parameters derived from its response could be used to predict curd moisture content throughout syneresis (standard error of prediction = 1.72% [w/w]; R^2 = 0.95) (Fagan and others 2008). Other studies have investigated an optical sensor to monitor casein particle size distribution in whey (Guillemin and others 2006) and ultrasonic velocity to determine the spontaneous onset of syneresis in a milk gel (Taifi and others 2006).

The curd–whey mixture can be regarded as a texture pattern that changes during processing as the volume of expelled whey increases and curd particles contract. In this study, 5 image texture analysis methods (FGLS, GLCM, RLM, FD, and WT) are evaluated for predicting curd moisture and whey solids during syneresis. The objectives of this study were to:

(1) Extract a range of image texture features from images captured during syneresis in a stirred laboratory-scale cheese vat.
(2) Determine if these features may be used to monitor syneresis.
(3) Employ these features in models to predict curd moisture content and solids in whey during syneresis.

Materials and Method

Experimental design and set-up

A fully randomized factorial experimental design was employed with 2 factors and 2 levels per factor ($N = 12$). The factors selected were milk pH at 6.0 and 6.5 and stirring speed during syneresis at 12.1 and 27.2 rpm. This design, which was carried out in triplicate, provided a range of coagulation and syneresis rates over which the potential of image texture features to monitor curd syneresis in a 11 L double-O cheese vat (Pierre Guerin Technologies, Mauze, France) was evaluated. The experimental procedure is outlined in Figure 1. Milk was coagulated using a fixed concentration of calcium chloride and rennet. The double-O cheese vat, as described by Everard and others (2007), had twin corotating stirrers with stirring blades set at a 30° angle and with 8- to 10-mm clearance from the base of the cheese vat. This resulted in a 3-D flow of curd–whey mixture representing commercial cheese making during stirring.

Milk preparation, coagulation, and cutting procedures

Low-fat pasteurized milk (Avonmore Slimline Milk, Glanbia, Ireland), with protein and fat contents of 38 and 3 g/L, respectively, was used in this study. The milk was prepared for coagulation according to the procedure of Everard and others (2007), which included adjustment of milk pH on the day prior to the experiment. On the day of the experimentation, 10 kg of milk were added to the cheese vat and heated to 32 °C with stirring at 27.2 rpm. A final adjustment of milk to the target pH, as per the experimental design, was carried out at 32 °C. The milk coagulant used was 100% recombinant chymosin (CHY-MAX extra, 600 IMCU/mL; Chr Hansen Ireland Ltd., Ireland). The rennet was added to the milk (0.18 g of chymosin per kilogram of milk) in the vat while being stirred constantly at 55 rpm. Stirring was stopped after 3 min, at which point the stirrers were replaced with twin cutting blades and a 3.5-mL aliquot of milk was removed from the vat and loaded into a controlled stress rheometer (Carri-med CSL^2-100, TA Instruments, U.K.). The instrument was operated at 32 °C in oscillation mode at a shear strain of 0.02 and a frequency of 1 Hz using double-gap concentric cylinder geometry. Cutting time (t_{cut}) was determined by the rheometer as the time at which the storage modulus (G') of the milk gel was 43 Pa as detailed by Everard and others (2007). At t_{cut} the twin cutting

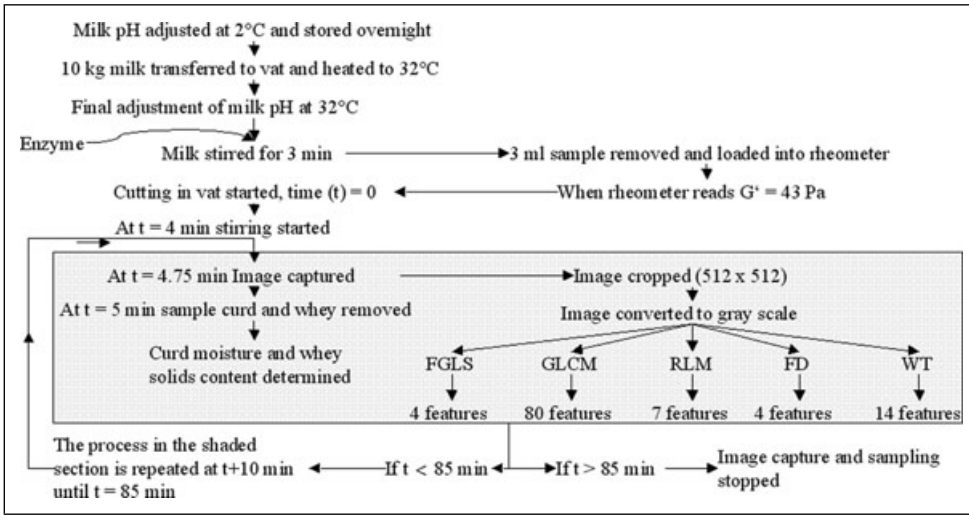

Figure 1—Flow diagram of the procedures employed for experimental trials and analysis, and extracting image texture features.

blades were activated and the gel was cut at a constant speed of 6 rpm for 15 s, then allowed to heal for 1 min, cut a 2nd time at a speed of 16 rpm for 15 s, allowed to heal for 1 min, and cut a 3rd time at speed 16 rpm for 10 s and allowed to heal for 1 min. The moment of initiating gel cutting was taken as the reference time ($t = 0$) for all subsequent measurements.

Compositional analysis of curd and whey

Samples of the curd–whey mixture (approximately 180 mL) were removed from the vat at 10 min intervals from $t = 5$ up to $t = 85$ min. Curd and whey were separated using a 75-μm stainless steel sieve (AGB, Dublin, Ireland), which ensured that whey fat globules were not retained by the sieve. Samples of approximately 3 g of curd and 5 g of whey were then accurately weighed into preweighed aluminum dishes for determination of total solids of curd and whey, respectively, by drying in triplicate in a convection oven at 102 °C for 16 h (Fagan and others 2007d). The solids in whey was expressed as grams of whey total solids per kilogram of whey.

Image preprocessing

All algorithms developed for preprocessing of full images and subsequent image texture analysis were written in MATLAB 6.5 (The MathWorks Inc., Mass., U.S.A.).

A computer vision system was used to capture images of the surface of the curd–whey mixture in the vat as outlined by Everard and others (2007). Figure 2 shows images of the surface of the curd–whey mixture captured at 4, 14, 24, and 34 min after gel cutting time. The central sections of the original images of size 720 × 574 pixels were cropped into square images (512 × 512 pixels) to facilitate wavelet-based texture analysis. This processing did not affect the conclusions of this study because the square images obtained were sufficiently large to capture the changes in curd and whey during syneresis. This also improved the robustness of the method by removing the most inhomogeneous parts of the image caused by reflection of light. The cropped square images were converted to gray scale by eliminating the hue and saturation information while retaining the luminance.

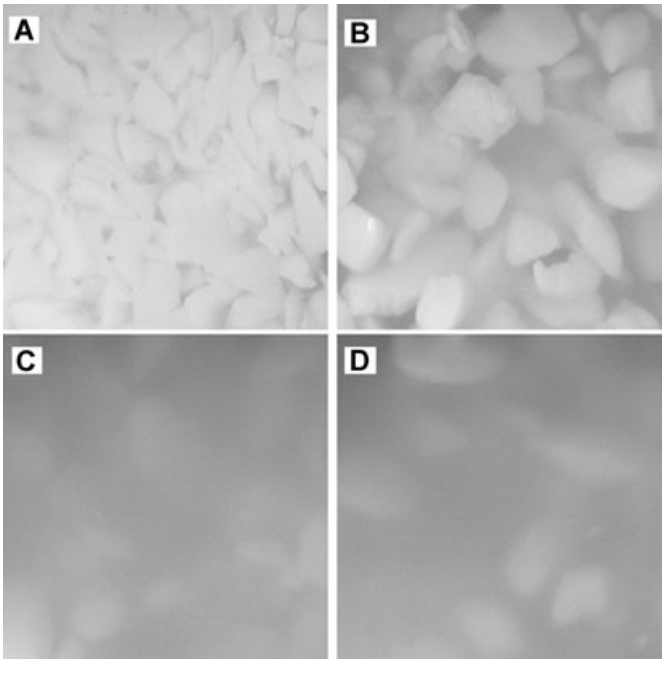

Figure 2—A sequence of images captured during the syneresis process at (A) 4, (B) 14, (C) 24, (D) 34 min after gel cutting time.

Image texture analysis

Preprocessed images were subjected to 5 image texture analysis techniques, namely FGLS, GLCM, RLM, FD, and WT.

First-order gray level statistic. FGLS is a 1st-order statistical method. Pixel histograms, that is, a count of how many pixels in an image possess a given gray level value, were obtained for each image. From each histogram, 4 features, namely, mean, variance, skewness, and kurtosis, were derived (Du and Sun 2006). FGLS considers the intensity of individual pixels but does so independently of neighboring pixels.

Gray level co-occurrence matrix. In contrast, GLCM is a 2nd-order statistical method; that is, it takes into account the spatial relationship between pixels. GLCM estimates the probability $P_d(i,j)$ that 2 pixels separated by a specified distance d and direction θ have gray levels i and j. GLCMs can be constructed with different distances and directions. Forty GLCMs were constructed with a distance value of 1 to 10 and angles of 0, 45, 90, and 135°. Eight features, namely, angular 2nd moment (ASM), sum of squares (SS), inverse difference moment (IDM), entropy, difference variance (DV), 2 information measures of correlation (IC1 and IC2), and cluster prominence (Cpromi), were derived from each GLCM as suggested by Haralick and others (1973) and Conners and others (1984). Average values derived from the 4 GLCMs with different directions (0, 45, 90, and 135°) were considered as the final values for each GLCM at a specific distance. This resulted in the extraction of 8 features at 10 distances, that is, 80.

Run-length matrix. The RLM approach is a technique for searching the image in a given direction for runs of pixels that have the same gray level value. For a given cheese image, a run-length matrix RLM (g, r) is defined as the number of runs with pixels of gray level g and run length r. Different run directions may be used for constructing RLMs. Two RLMs were constructed with the run directions of 0 and 90°. Seven features, short-run emphasis (SRE), long run emphasis (LRE), gray level nonuniformity (GLN), run-length nonuniformity (RLN), run-length percentage (RLP), and low and high gray level run emphases (LGRE, SGRE), as proposed by Galloway (1975) and Chu and others (1990), were computed from each RLM. The final results were calculated by averaging the 2 values obtained from the 2 RLMs.

Fractal dimension. Traditional methods for image texture analysis, such as GLCM and RLM, are limited in that they are restricted to the analysis of an image over a single scale. FD, however, is a multiscale analysis technique. The FD approach relies on the concept of self-similarity such that an object is self-similar only if that object can be broken down into an arbitrary number of smaller sections, each of which is a replica of the entire structure. The differential box counting method presented by Sarkar and Chaudhuri (1994) was applied to describe FD texture features. Each image is viewed as a hilly terrain whose height at any given location is proportional to the gray level value at that location. Therefore, considering the gray level values to be heights protruding above a plane, the image can be treated as a rugged surface. The image is then partitioned by overlaying it with a grid. The resulting boxes are numbered sequentially according to intensity, from one up to the box containing the highest intensity, and the number of self-similar pieces can be calculated according to the method of Chaudhuri and others (1993). By repeating this process using a number of different grid sizes, the FD can be estimated from the slope of the linear regression between a logarithmic plot of the number of self-similar

pieces versus the relative grid scale. The original image was transformed to provide 3 images, the original and the high gray level and low gray level images. Four fractal texture features were extracted from them, including FDs of the original (FDO), the high gray level (FDHGL) and the low gray level images (FDLGL), and the multifractal of order 2 (FDM), which is calculated from the original image (Chaudhuri and others 1993).

Wavelet transform. WT is another well-known multiscale analysis technique that is useful for characterizing different scales of textures effectively. Using the steerable pyramid transform developed by Simoncelli and Freeman (1995), a pair of filters, 1 high-pass and 1 low-pass, were initially applied to the image. The low-pass image was then further decomposed into a set of 12 sub-bands and a final low-pass image. The 12 orientated sub-bands comprised 3 scale levels and 4 orientation bands (that is, $3 \times 4 = 12$). Figure 3 illustrates an example of the decomposition of a cheese image. The WT texture features were computed as the energies of the high-pass image (HPVE), final low-pass image (LPVE), and each of the 12 sub-band images, where LmBnE is the energy of the sub-band at the *m*th scale level and the *n*th orientation band, which is widely used for wavelet-based texture characterization (Kokare and others 2004).

Statistical analysis

Correlation analysis was carried out using the CORR procedure of SAS statistical software (version 9.1, 2002 to 2003, SAS Inst., Cary, N.C., U.S.A.) to examine the relationship between image texture features and composition of the curd and whey mixture in the cheese vat. This relationship as well as the relationship between image texture features was further studied using multivariate analysis by partial least squares (PLS) regression, which was carried out using The Unscrambler software (v.9.6; Camo A/S, Oslo, Norway).

Finally, regression models for predicting curd moisture content (C_M) and solids in whey (S_W) were developed using the REG procedure and MAXR model-selection method in SAS. Separate models were developed for each of the 5 image texture analysis methods. Time from cutting was included as a variable due to the significant impact it will have on syneresis. The MAXR model-selection method develops models with the largest R^2 by examining all possible combinations of the variables selected for modeling. The Akaike information criterion (AIC) was used to select the best models for predicting C_M and S_W. The practical utility of the final models was also assessed by calculating the range error ratio (RER) (Williams 2001). This ratio is calculated by dividing the range of a given parameter by the prediction error for that parameter. Models with an RER of less than 3 have little practical utility; RER values of between 3 and 10 indicate limited to good practical utility, and above 10, the model has a high utility value (Williams and Norris 1987). The accuracy of the models was also evaluated based on the coefficients of determination (R^2) for predicted versus measured attributes: R^2 between 0.50 and 0.65 indicates that discrimination between high and low values can be made, R^2 between 0.66 and 0.81 indicates approximate quantitative prediction, whereas R^2 between 0.82 and 0.90 reveals good prediction. Models having R^2 above 0.91 are considered to be excellent (Williams 2003).

Results and Discussion

Correlation analysis

It is clear from Figure 2 that during syneresis the contents of the cheese vat proceeds from a predominantly white mass to a mixture of white particles suspended in yellow liquid whey to an almost continuous mass of yellowish whey. This is due to the contraction of the curd particles and the associated expulsion of whey. Solids comprising fat and fines will also be expelled in the whey. To produce a high quality cheese product, curd moisture content and solids retention, which are functions of the rate and extent of syneresis, must be optimized. Therefore curd moisture content (C_M), which decreases during syneresis, and the solids content in whey (S_W), which increases during syneresis, were selected as 2 indices of syneresis.

The 1st step in determining the suitability of the extracted image features to monitor curd syneresis in a stirred cheese vat was to carry out a simple correlation analysis. Therefore, C_M and S_W were correlated with the 109 parameters extracted from the images captured at each sampling time point. This correlation analysis allowed for a preliminary assessment of the relationship between syneresis kinetics and the image texture features. Table 1 shows that strong significant correlations were observed between the 2 indices of syneresis and a number of image texture features.

Of the image texture analysis methods studied, FGLS had the lowest number of features highly correlated ($P < 0.01$) with C_M and

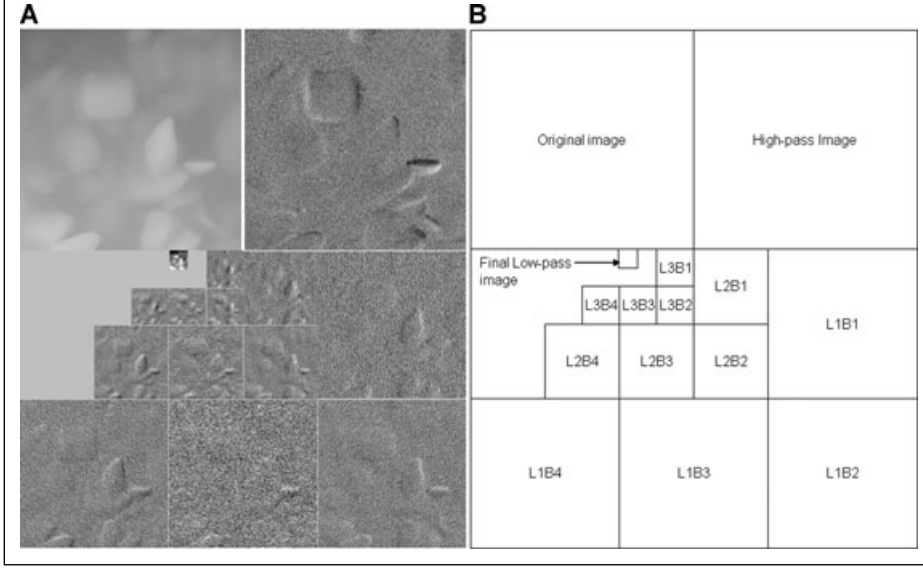

Figure 3—(A) Decomposition of a cheese image showing the original image, high-pass image, 12 sub-band images at each scale and orientation, and the final low-pass image; and (B) a schematic of the process showing the coding system: LmBn is the sub-band at the *m*th scale level and the *n*th orientation band.

S_W. In fact, mean was the only FGLS feature to meet this criterion. This may be due to the limitation of these 1st-order statistics in which they are only representative of individual pixel intensities and not their relative location within the image. As C_M decreases, curds particles shrink and occupy a smaller area of the image. Hence the average pixel intensity gray level decreases, resulting in mean being positively correlated with C_M and negatively correlated with S_W.

Initial results suggested that the GLCM features calculated at distances of 3 and 4 were most significantly correlated with C_M and S_W, respectively. Therefore, only GLCM features extracted at these distances will be further discussed. Table 1 presents the correlation between GLCM features extracted at distance 3 and C_M and at distance 4 and S_W. GLCM features tended to be more correlated to S_W than C_M. ASM was positively correlated with S_W. ASM measures the gray level differences that can be used to describe relative smoothness and is therefore a measure of image uniformity. A low ASM value indicates a high variation in gray level, that is, low uniformity, while a high ASM indicates high image uniformity. When the milk gel is cut (time = 0 min), the image will be highly uniform with little variance in gray levels because it is composed mainly of curd. In subsequent images, uniformity decreases with the progression of syneresis as a mixture of curd and whey is observed. However, at a certain point during syneresis, whey becomes the dominant component of the images, which results in a more uniform texture. SS is a measure of the roughness of the image, which will decrease during syneresis as curd particles become more dispersed in whey, and hence is positively and negatively correlated with C_M and S_W, respectively. Entropy is an indication of the degree of order in an image and behaves in a similar but opposing manner to ASM; that is, the randomness in images initially increases during syneresis but will eventually decrease as less curd is observed at the surface of the vat. Hence, entropy is negatively correlated with S_W. DV, which was negatively correlated with S_W, relates to the heterogeneous distribution of features in the image, which decreases during syneresis. DV was the GLCM parameter with highest correlation to S_W ($R = -0.78$). IC2 is an information measure of correlation, that is, the linear dependencies of gray level values in an image. The linear dependence between gray levels will increase during syneresis as the images become more homogenous, that is, predominately composed of whey and, hence, IC2 and S_W were positively correlated. Cpromi is a measure of skewness or lack of symmetry. When Cpromi is high, the image is not symmetric. Therefore Cpromi increases immediately after cutting followed by a subsequent decrease, hence the negative correlation with S_W and the weakly positive correlation with C_M.

The majority of RLM features were correlated with C_M but the relationships were very weak ($R = 0.27$ to 0.31). LGRE, which measures the distribution of low gray level values, was the RLM feature of most interest due to its stronger correlation with S_W ($R = -0.65$). LGRE and the 1st-order statistic mean were closely related ($R = 0.997$), hence, the similar relationship between these features and C_M and S_W.

The FD of an image is an indication of the roughness of the image at different scales. FDO increased during syneresis and was the FD feature as well as the overall image texture feature investigated in this study with the highest correlation to C_M ($R = -0.64$) and S_W ($R = 0.84$).

The wavelet energies associated with the 12 sub-band images obtained by WT are measures of the frequency content of the image on a given scale and in a given direction. With the exception of L1B3E, these features, that is, L1B1E to L3B4E, are all similarly correlated to C_M and S_W. Hence only L1B1E to L1B4E are shown in Table 1. The wavelet energies associated with those 11 sub-band images and the final low-pass image (LPVE) were all positively correlated with C_M ($R = 0.41 \pm 0.05$) and negatively correlated with S_W ($R = 0.73 \pm 0.08$).

FD and WT features exhibited some of the highest correlations with C_M and S_W. As both FD and WT characterize the scaling properties of the image, it indicates that image texture features of multiscale representations are most strongly correlated with syneresis.

Partial least squares regression analysis

PLS regression involves the compression of the X matrix, that is, the image texture features, to a few new variables, called components, which are linear combinations of the original data. Each variable is related to each component by its loading value. Analysis of the PLS scatter plot of the X- and Y-loading facilitates the detection of important predictors and the understanding of the relationships between the X and Y variables. Hence, PLS regression was carried out using 45 image texture features (X variables) and syneresis indices C_M and S_W (Y variables). The image texture features used were the 4 FGLS features, 16 GLCM features (that is, 8 features at distances 3 and 4), 7 RLM features, 4 FD features, and 14 WT features.

Table 1—Significance of correlation between curd moisture content (C_M), solids in whey (S_W), and the extracted image texture features.

FGLS features	Mean	Variance	Skewness	Kurtosis				
C_M	**	—	—	—				
S_W	***	*	—	*				
GLCM features	ASM	SS	IDM	Entropy	DV	IC1	IC2	Cpromi
C_M	—	***	—	—	—	—	—	*
S_W	***	***	***	***	***	—	***	**
RLM features	SRE	LRE	GLN	RLN	RP	SGRE	LGRE	
C_M	**	**	—	**	**	—	**	
S_W	—	—	*	—	—	—	***	
FD features	FDO	FDHGL	FDLGL	FDM				
C_M	***	*	—	***				
S_W	***	—	—	*				
WT features	HPVE	L1B1E	L1B2E	L1B3E	L1B4E	LPVE		
C_M	**	***	***	**	***	***		
S_W	—	***	***	**	***	***		

$^{***}P < 0.001$, $^{**}P < 0.01$, $^{*}P < 0.05$, — = not significant; $N = 108$.
See Nomenclature for definition of image texture features.

Due to the large difference in magnitude and variability between image texture features, it was necessary to standardize them to unit variance prior to investigating their inter-relationships. In the loadings, plot for standardized image texture features, C_M and S_W for components 1 and 2, component 1 explained 45% of the variation in the image texture feature data and 19% of the variation in the C_M and S_W data, while component 2 explained 36% of the variation in the image texture feature data and 16% of the variation in the C_M and S_W data (Figure 4). Parameters located close to each other in the loadings plot are similar with respect to components 1 and 2. For example, RP, RLN, and SRE are all located in very close proximity at the negative extreme of component 2, indicating high correlations. Likewise, with the exception of HPVE, all the WT-based textural features are clustered in a small region at the positive extreme of component 1. As expected for the correlation analyses, the energies of a number of the sub-bands are very closely related. Despite this clustering, the image texture features are widely distributed throughout the loadings plot, suggesting that different features are providing a variety of information. However, parameters located close to the origin, such as SGRE, skewness, and $IC1_3$ and $IC1_4$ (where subscripts denote the distance at with the GLCM features were extracted), are not well represented in the plot and cannot be interpreted.

C_M and S_W, highlighted in bold in Figure 4, are somewhat diagonally opposed to each other. The central location of C_M in the positive region of both component 1 and 2 suggests that the variation in C_M is accounted for by both components. However, S_W, with its large negative loading along component 1 but smaller negative loading along component 2, is mostly explained by component 1. It is also interesting to note the image texture features that are located close to C_M and S_W. FDO was located close to S_W and in opposition to C_M, confirming results of the correlation analysis, where S_W and C_M were positively and negatively correlated with FDO, respectively. In relation to component 1, which does account for the majority of the variation in the data, S_W is also positively related to FDLGL and $IC2_4$ and negatively related to the parameters that dominate the positive extreme of component 1 (WT subband energy features, DV_4, SS_3, and SS_4). C_M, like S_W, is also closely related to parameters that dominate the positive and negative extremes of component 1; however, the relationship between C_M and these parameters is weaker.

Overall PLS regression confirmed the results of the correlation analysis. All features located in the negative half of component 1 were previously found to be positively related to S_W. All features located in the positive half of component 1 were positively correlated to C_M, with the exception of the features located at the negative extreme of component 2 (RP, RLN, SRE, FDM, HPVE). However, the distribution of features in Figure 4 suggests that different image texture analysis methods may be capturing different information.

Prediction of curd moisture and whey solids using image texture features

The results of the correlation and PLS regression analysis indicated that a small number of image texture features have limited or no relationship with C_M or S_W. These parameters were identified as those having no significant correlation with either C_M or S_W in Table 1, and a location close to the origin in Figure 4. Three parameters, SGRE, skewness, and IC1, met these criteria and were therefore not included in any further analysis. PLS regression also revealed that some of the GLCM features extracted using distances 3 and 4 were highly correlated, such as SS_3 and SS_4. Therefore, the GLCM features extracted using distance 3 were used to predict C_M and those extracted using distance 4 were used to predict S_W. The models developed using each of the image texture analysis methods are given in Table 2 for C_M and Table 3 for S_W. In both cases, the FGLS and FD models contained the smallest number of terms

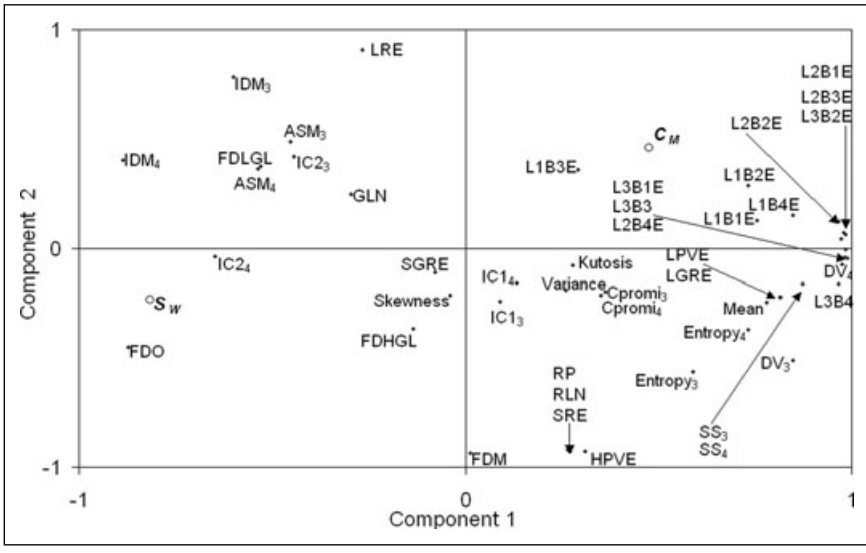

Figure 4—Partial least squares regression loadings plot of the extracted image texture features, curd moisture and solids in whey, of principal components 1 and 2. See Nomenclature for definition of image texture features.

Table 2—Models for the prediction of curd moisture content (C_M) (% (w/w)) using independent variables and extracted image texture features.

Model nr	Technique	R^2	SEP% (w/w)	Variables in model							
I	FGLS	0.62	1.20	Time	Mean	Skewness	Kurtosis				
II	GLCM	0.79	0.90	Time	Contrast	SS	IDM	SA	SV	Entropy	DE
III	RLM	0.72	1.04	Time	SRE	LRE	GLN	RP			
IV	**FD**	**0.72**	**1.03**	**Time**	**FDO**	**FDLGL**	**FDM**				
V	WT	0.71	1.06	Time	HPVE	L1B1E	L1B3E	L3B4E			

See Nomenclature for definition of image texture features.

Table 3—Models for the prediction of solids in whey (S_W) (grams per kilogram), using independent variables and extracted image texture features.

Model nr	Technique	R^2	SEP (g/kg)	Variables in model						
VI	FGLS	0.61	0.82	Time	Mean	Skewness	Kurtosis			
VII	GLCM	0.79	0.60	Time	ASM	SS	SA	SV	Entropy	Cpromi
VIII	RLM	0.76	0.64	Time	LRE	GLN	RLN	RP	LGRE	
IX	FD	**0.80**	**0.58**	**Time**	**FDO**	**FDLGL**	**FDM**			
X	WT	0.81	0.58	Time	HPVE	L1B1E	L1B3E	L1B4E	L2B1E	

See Nomenclature for definition of image texture features.

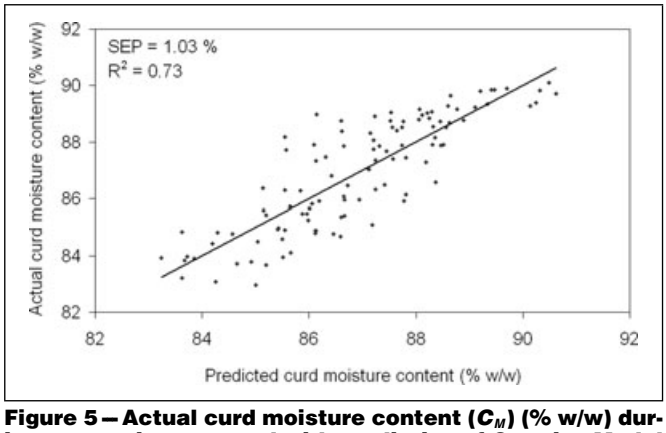

Figure 5—Actual curd moisture content (C_M) (% w/w) during syneresis compared with prediction of C_M using Model IV (Table 2). R^2 = coefficient of determination; SEP = standard error of prediction.

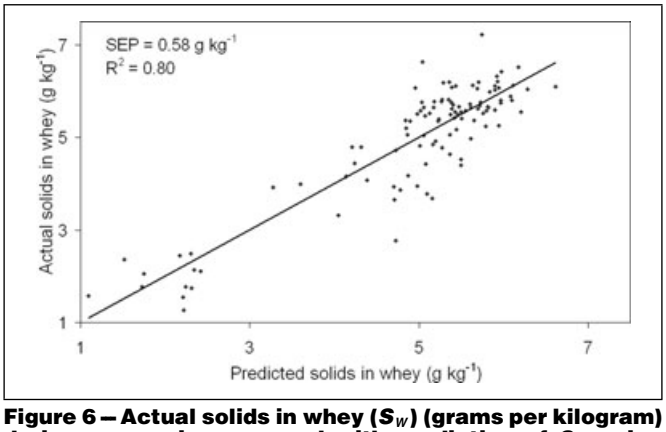

Figure 6—Actual solids in whey (S_W) (grams per kilogram) during syneresis compared with prediction of S_W using Model XI (Table 3). R^2 = coefficient of determination; SEP = standard error of prediction.

(4), indicating that they should be more robust than the models developed using parameters from the other image texture analysis methods. However, the FD models were significantly more accurate than the FGLS models. Indeed, the FD models had the lowest AIC values and thus the FD models were the best methods for predicting C_M and S_W during syneresis. The FD model (model IV) predicted C_M with an SEP of 1.03% (w/w) and a R^2 of 0.72, indicating that this model provided approximate quantitative prediction (Figure 5). The RER of 7 for this model also indicated a good practical utility. The S_W FD model (model IX) also gave approximate quantitative prediction ($R^2 = 0.80$) with an SEP of 0.58 g/kg (Figure 6). However, the RER was higher (RER = 10), suggesting the model has a high utility value. The 2nd best technique for predicting syneresis indices was WT, followed by GLCM, RLM, and, finally, FGLS. This confirms that the "global description" provided by the FGLS features is not adequate to monitor syneresis. Features extracted by GLCM and RL give a better description of the local structure within the image; hence they provided better predictions than FGLS. The GLCM technique was previously found to have better performance than RLM as the latter was greatly influenced by noise (Conners and Harlow 1980). However, more storage elements and computation are required for the GLCM method. The FD and WT models have the advantage that they are multiscale techniques and take into account the entire image. The application of WT in the food industry has been limited, probably due to its requirement for the processing region to be square. However, in the current application, this is not a major limitation. In general, the advantage of the FD method over other image texture analysis methods is that it can be used to describe highly irregular images. However, the corresponding disadvantage is that multidimensional features are required to describe an image with inhomogeneous scaling properties and the computation of such features takes longer.

There has been only 1 other study that examined the potential of a computer vision system to monitor curd syneresis (Everard and others 2007). They utilized 2 image analysis techniques, that is, the change in the average RGB values of the images during syneresis and the change in the ratio of the area of curd to whey (a_{wy}), in which a threshold value between curd and whey was determined by human perception. However, the models presented in Table 2 and 3 are a significant improvement on those reported by Everard and others (2007). They developed models using pH, stirring speed, and a parameter relating to the change in RGB values during syneresis. They predicted C_M with an SEP of 1.29% (w/w) ($R^2 = 0.61$) and S_W with an SEP of 0.83 g/kg ($R^2 = 0.53$). They also found that C_M at high stirring speeds could be predicted ($R^2 = 0.92$) by an equation comprising an intercept and 4 variables, that is, time, time^2, and 2 parameters derived from the evolution of a_{wy} during syneresis. However, Everard and others (2007) found that no prediction was possible at low stirring speeds. The low stirring speed confounded the prediction due to the level of curd particles kept in suspension at the surface of the vat. The FD models (models IV and IX) did not display the considerable confounding effect of low stirring speeds on predictions accuracy as found by Everard and others (2007). This indicates that the novel features extracted by image texture analysis may be more appropriate for monitoring curd syneresis than the RGB and a_{wy} method.

Fagan and others (2008) have also developed a model for predicting C_M during syneresis, using process parameters and parameters from a light backscatter sensor, with an SEP of 1.72% (w/w) ($R^2 = 0.95$, RER = 23). Therefore, further study of the proposed technique over a wider range of coagulation and syneresis rates is required to provide a more precise method of monitoring syneresis.

Effect of pH and stirring speed on selected image texture features

It is widely accepted that syneresis follows 1st order kinetics (Castillo and others 2006; Fagan and others 2007c). Consequently the evolution of parameters extracted by image texture analysis

during syneresis should ideally follow 1st order kinetics if they are to have potential for monitoring syneresis. To evaluate this hypothesis, 4 image texture features from the top 2 models for predicting C_M (models IV and V) and S_W (models IX and X) (Table 2 and 3) were fitted to a 1st order equation (Eq. 1) as described by Fagan and others (2007c) using the PROC NLIN procedure in SAS.

$$IF_t = IF_\infty + (FI_5 - IF_\infty)e^{-kt} \quad (1)$$

where IF_t was the image texture feature at time t (min), IF_∞ was the image texture feature at an infinite time, FI_5 was the image texture feature at $t = 5$ min, and k was the kinetic rate constant (per minute) for changes in the image texture feature during syneresis. The parameters selected were the most significant features in each of the selected models (models IV, V, IX, X). These features were FDO, FDLGL, L1B1E, and HPVE. The correlation between fitted and experimental data was excellent ($R = 0.89$ to 0.995). It can be concluded that the change in image texture features followed 1st-order kinetics, as shown by fitting of 1st-order equations to FDO experimental data recorded during syneresis (Figure 7). Analysis of variance on the effect of pH and stirring speed on the kinetic rate constants (k) of FDO, FDLGL, L1B1E, and HPVE showed that pH had the greatest effect on the rate of change of FDLGL and HPVE, that is, k FDLGL and k HPVE ($P < 0.01$). Stirring speed, however, significantly affected the rate of change of FDO and FDLGL, that is, k FDO and k FDLGL ($P < 0.001$) (Table 4).

Conclusions

A total of 109 image texture features were extracted by 5 image texture analysis techniques. They were extracted by FGLS (4 features), GLCM (80 features, 8 features at 10 distances), RLM (7 features), FD (4 features), and WT (14 features) procedures. The potential of these features for monitoring syneresis was investigated. It was concluded that the FD models were the best for predicting curd moisture and the level of solids in whey during syneresis. The 2nd best technique for predicting syneresis indices was WT. This indicates that multiscale analysis techniques such as FD and WT extracted the most relevant information from images captured during syneresis. The FD models predicting curd moisture and solids in whey with standard errors of prediction of 1.03% (w/w) and 0.58 g/kg, respectively. The application of such a technique in the future may facilitate greater control of curd moisture content and yield, thereby facilitating the production of higher quality and more consistent cheese products.

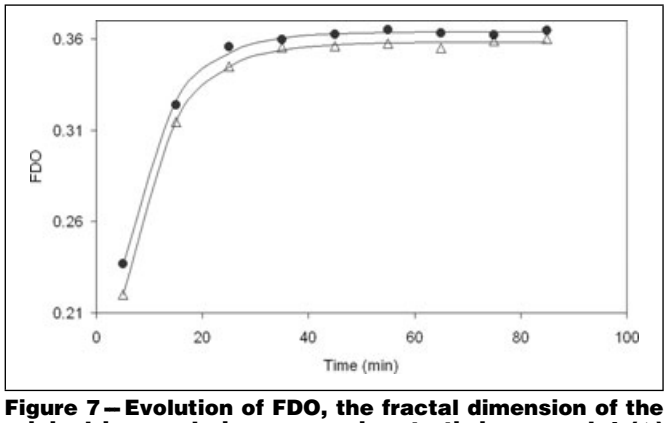

Figure 7—Evolution of FDO, the fractal dimension of the original image during syneresis, at stirring speed 4 (Δ) and 2.5 (•) and pH 6. Time zero corresponds to the gel cutting time. Theoretical curve (—) assuming 1st order kinetics. Each data point is an average of 3 replicates.

Table 4—Analysis of variance showing the effects of pH and stirring speed on the kinetic rate constants (k) of FDO, FDLGL, L1B1E, and HPVE.

Source	DF	k FDO	k FDLGL	k L1B1E	k HPVE
pH	1	*	**	—	**
Speed	1	***	***	—	—

Speed = stirring speed; *** $P < 0.001$, ** $P < 0.01$, * $P < 0.05$, — = not significant; DF = degrees of freedom.
See Nomenclature for definition of image texture features.

Acknowledgments

This research has been funded by the Food Institutional Research Measure (FIRM), administered by the Irish Dept. of Agriculture and Food.

Nomenclature

ASM	angular second moment
C_M	curd moisture content
Cpromi	cluster prominence
CS	cluster shade
DV	difference variance
FD	fractal dimension
FDHGL	FD of the high gray level image
FDLGL	FD of the low gray level image
FDM	multifractal of order 2
FDO	FD of the original image
FGLS	first-order gray level statistics
FT	Fourier transform
GLCM	gray level co-occurrence matrix
GLN	gray level nonuniformity
HPVE	energy of the high-pass residual band
IC	information measures of correlation
IDM	inverse difference moment
LGRE	low gray level run emphases
LmBnE	energy of the sub-band at the mth pyramid level and the nth orientation band
LPVE	energy of the low-pass residual band
LRE	long-run emphasis
PLS	partial least squares
RER	range error ratio
RGB	red, green, and blue
RLM	run-length matrix
RLN	run-length nonuniformity
RLP	run-length percentage
SEP	standard error of predictions
SRE	short-run emphasis
SS	sum of squares
S_W	solids in whey
WT	wavelet transform

References

Apostolopoulos C, Marshall RJ. 1994. A quantitative method for the determination of shreddability of cheese. J Food Qual 17:115–28.
Blazquez C, Downey G, O'Donnell C, O'Callaghan D, Howard V. 2004. Prediction of moisture, fat and inorganic salts in processed cheese by near infrared reflectance spectroscopy and multivariate data analysis. J Infrared Spectrosc 12(3):149–57.
Castillo M, Lucey JA, Wang T, Payne FA. 2006. Effect of temperature and inoculum concentration on gel microstructure, permeability and syneresis kinetics. Cottage cheese-type gels. Int Dairy J 16(2):153–63.
Chaudhuri BB, Sarkar N, Kundu P. 1993. Improved fractal geometry based texture segmentation technique. IEE Proc-Comp Digit Tech 140(5):233–41.
Chu A, Sehgal CM, Greenleaf JF. 1990. Use of grey value distribution of run lengths for texture analysis. Pattern Recognit Lett 11:415–20.

Conners RW, Harlow CA. 1980. A theoretical comparison of texture algorithm. IEEE Trans Pattern Anal Mach Intell 2:204–22.
Conners RW, Trivedi MM, Harlow CA. 1984. Segmentation of a high-resolution urban scene using texture operators. Comput Vision Graph Image Process 25:273–310.
Du CJ, Sun D-W. 2004. Recent developments in the applications of image processing techniques for food quality evaluation. Trends Food Sci Technol 15(2):230–49.
Du CJ, Sun DW. 2006. Correlating image texture features extracted by five different methods with the tenderness of cooked pork ham: a feasibility study. Trans ASABE 49(2):441–8.
Emmons DB. 1993. Variability of moisture content in Cheddar cheese. Cheese yield and factors affecting its control. In: IDF seminar. Brussels, Belgium: Intl. Dairy Federation. p 293–301.
Everard CD, Fagan CC, O'Donnell CP, O'Callaghan DJ, Castillo M, Payne FA. 2007. Computer vision and colour measurement techniques for inline monitoring of cheese curd syneresis. J Dairy Sci 90:3162–70.
Fagan CC, Castillo M, Payne FA, O'Donnell CP, O'Callaghan DJ. 2007a. Effect of cutting time, temperature and calcium on curd moisture, whey fat losses and curd yield by response surface methodology. J Dairy Sci 90:4499–512.
Fagan CC, O'Donnell CP, O'Callaghan DJ, Downey G, Sheehan EM, Delahunty CM, Everard C, Guinee TP, Howard V. 2007b. Application of mid-infrared spectroscopy to the prediction of maturity and sensory texture attributes of Cheddar cheese. J Food Sci 72(3):E130–7.
Fagan CC, Castillo M, Payne FA, O'Donnell CP, Leedy M, O'Callaghan DJ. 2007c. Novel online sensor technology for continuous monitoring of milk coagulation and whey separation in cheese making. J Agric Food Chem 22:8836–44.
Fagan CC, Leedy M, Castillo M, Payne FA, O'Donnell CP, O'Callaghan DJ. 2007d. Development of a light scatter sensor technology for online monitoring of milk coagulation and whey separation. J Food Eng 83(1):61–7.
Fagan CC, Castillo M, O'Donnell CP, O'Callaghan DJ, Payne FA. 2008. Online prediction of cheese making indices using backscatter of near infrared light. Int Dairy J 18:120–8.
Galloway MM. 1975. Texture analysis using gray level run length. Comput Graph Image Process 4:172–9.
Guillemin H, Trelea IC, Picque D, Perret B, Cattenoz T, Corrieu G. 2006. An optical method to monitor casein particle size distribution in whey. Lait 86(5):359–72.
Haralick RM, Shanmugan K, Dinstein I. 1973. Textural features for image classification. IEEE Trans Syst Man Cybern B Cybern 3(6):610–21.
Jeliński T, Du C-J, Sun D-W, Fornal J. 2007. Inspection of the distribution and amount of ingredients in pasteurized cheese by computer vision. J Food Eng 83(1):3–9.
Kokare M, Chatterji BN, Biswas PK. 2004. Cosine-modulated wavelet based texture features for content-based image retrieval. Pattern Recognit Lett 25(4):391–8.
Li J, Tan J, Martz FA, Heymann H. 1999. Image texture features as indicators of beef tenderness. Meat Sci 53:17–21.
Li J, Tan J, Shatadal P. 2001. Classification of tough and tender beef by image texture analysis. Meat Sci 57:341–6.
Majumdar S, Jayas DS. 2000. Classification of cereal grains using machine vision. III. Texture models. Trans ASABE 46(6):1681–7.
McCauley JD, Thane BR, Whittaker AD. 1994. Fat estimation in beef ultrasound images using texture and adaptive logic networks. Trans ASABE 37(3):997–1002.
Mendoza F, Aguilera JM. 2004. Application of image analysis for classification of ripening bananas. J Food Sci 69(9):E471–7.
Misimi E, Mathiassen JR, Erikson U. 2007. Computer vision-based sorting of atlantic salmon (*Salmo salar*) fillets according to their color level. J Food Sci 72(1):S030–5.
Ni H, Gunasekaran S. 1995. A computer vision system for determining quality of cheese shreds. Food Processing Automation IV Proceedings of the FPAC Conference. St. Joseph, Mich.: ASAE.
Park B, Chen YR. 1996. Multispectral image co-occurrence matrix analysis for poultry carcasses inspection. Trans ASABE 39(4):1485–91.
Quevedo R, Carlos LG, Aguilera JM, Cadoche L. 2002. Description of food surfaces and microstructural changes using fractal image texture analysis. J Food Eng 53(4):361–71.
Sarkar N, Chaudhuri B. 1994. An efficient differential box counting approach to compute fractal dimension of images. IEEE Trans Syst Man Cybern B Cybern SMC 24:115–20.
Shiranita K, Miyajima T, Takiyama R. 1998. Determination of meat quality by texture analysis. Pattern Recognit Lett 19:1319–24.
Simoncelli EP, Freeman WT. 1995. The steerable pyramid: a flexible architecture for multi-scale derivative computation. Washington, D.C. p 444–7.
Taifi N, Bakkali F, Faiz B, Moudden A, Maze G, Décultot D. 2006. Characterization of the syneresis and the firmness of the milk gel using an ultrasonic technique. Meas Sci Technol 17(2):281–7.
Wang HH, Sun DW. 2002. Correlation between cheese meltability determined with a computer vision method and with Arnott and Schreiber tests. J Food Sci 67(2):745–9.
Whittaker AD, Park B, Thane BR, Miller RK, Savell JW. 1992. Principles of ultrasound and measurement of intramuscular fat. J Anim Sci 70:942–52.
Williams P. 2003. Near-infrared technology: getting the best out of light. A short course in the practical implementation of near infrared spectroscopy. Nanaimo, Canada. 109 p.
Williams PC. 2001. Implementation of near-infrared technology. In: Williams P, Norris K, editors. Near infrared technology in the agriculture and food industries. 2nd ed. St. Paul, Minn.: American Assoc. of Cereal Chemists Inc. p 164–5.
Williams P, Norris K. 1987. Implementation of near-infrared technology. In: Williams P, Norris K, editors. Near-infrared technology in the agricultural and food industries. St. Paul, Minn.: AACC. p 143–67.
Woodcock T, Fagan CC, O'Donnell CP, Downey G. 2008. Application of near andmid-infrared spectroscopy to determine cheese quality and authenticity. Food Bioprocess Technol 1:117–27.